ACS OMEGA

http://pubs.acs.org/journal/acsodf

Article

Novel Synergistic Process of Impurities Extraction and Phophogypsum Crystallization Control in Wet-Process Phosphoric Acid

Ganyu Zhu, Yunrui Yang, Lei He, Huiquan Li,* Ziheng Meng, Guangming Zheng, Fang Li, Xiaodan Su, Benjun Xi, and Zhongjun Li

Cite This: *ACS Omega* 2023, 8, 28122−28132

Read Online

ACCESS | Metrics & More | Article Recommendations

ABSTRACT: Phosphogypsum, as a byproduct of wet-process phosphoric acid reaction, has caused many environmental pollution problems. To improve the property and purity of phosphogypsum in the wet-process phosphoric acid process, a liquid−solid−liquid three-phase acid hydrolysis synergistic extraction reaction system was established by adding a certain amount of extractant in the actual production process. In order to study the extraction effect and residue of impurities in the reaction system, the phase, morphology, and impurity occurrences of phosphogypsum were systematically analyzed. The results showed that when the reaction time was 7 h, the reaction temperature was 80 °C, the reaction speed was 200 r/min, the volume ratio of the extractant to diluent (dilution ratio) was 1:4 and the volume ratio of the oil phase/aqueous phase (O/A ratio) was 1:1, P_2O_5 conversion was the highest in phosphate rock, and the residual P_2O_5 content in phosphogypsum was as low as 0.36%. The morphology of the phosphogypsum crystal was uniform and coarse long strip. The main forms of residual impurities were silicate, aluminum fluoride with crystal water, aluminate, phosphate, and fluoride. Meanwhile, the residual amount of main impurities in phosphogypsum was significantly reduced. Through this novel method, the property of phosphogypsum can be improved through the generation process and is greatly beneficial for its utilization and the recycling development of the wet-process phosphoric acid industry.

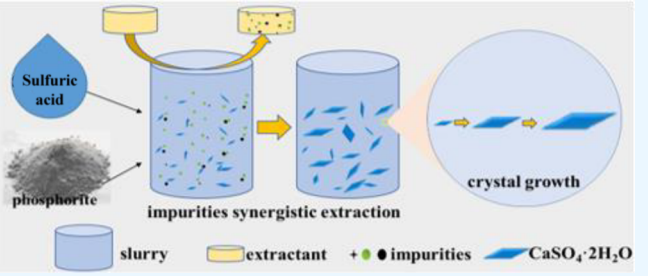

1. INTRODUCTION

Wet-process phosphoric acid (WPA) mainly refers to the process of phosphorus ore decomposition to phosphoric acid with sulfuric acid, and it is widely used to produce fertilizers and other phosphorous materials.[1,2] With the development of new energy industry, the utilization of battery materials such as lithium iron phosphate leads to the development of phosphoric acid. However, phosphogypsum with the main phase of calcium sulfate dihydrate ($CaSO_4 \cdot 2H_2O$) is also generated in this process as a byproduct, and 5 tons of phosphogypsum are emitted for every 1 ton of phosphoric acid produced. At present, phosphogypsum is growing worldwide at the rate of 200 million tons per year, and the comprehensive utilization rate is only 10−15%. The low utilization rate and the large stockpile of phosphogypsum lead to serious environmental pollution,[3,4] which is the core restriction for the development of WPA.

P_2O_5 in phosphogypsum entrained from the WPA process, which may release into the surroundings, is the most important restriction for its utilization. The contents of P_2O_5 in phosphogypsum may affect its crystallization. In the process of sulfuric acid hydrolysis, large amounts of impurities in the phosphorus ore enter into the reaction system. The existence of the impurities may affect the crystal growth of phosphogypsum, and the shape and size of the calcium sulfate crystal are the key factors that directly affect the filtration performance and residual phosphorus content of phosphogypsum. To date, many scholars have investigated the effect of impurities in phosphogypsum on the nucleation and growth of calcium sulfate.[5−7] The results show that Na^+ and K^+ in the system may change the morphology of the calcium sulfate crystal from the strip crystal to the needle crystal and decrease the aspect ratio.[8,9] Mg^{2+} ions enter the crystal structure and reduce the growth rate of calcium sulfate crystals, resulting in the increase of the aspect ratio of calcium sulfate and the growth of slender needle crystals.[10,11] Al^{3+} and Fe^{3+} can inhibit

Received: February 21, 2023
Accepted: May 3, 2023
Published: July 27, 2023

Table 1. Composition of Phosphate Rock

compound percent, wt %	CaO	P_2O_5	SiO_2	Al_2O_3	MgO	K_2O	Fe_2O_3	Na_2O	F
phosphate rock	48.48	29.41	10.57	2.93	1.09	1.31	0.93	0.40	2.97

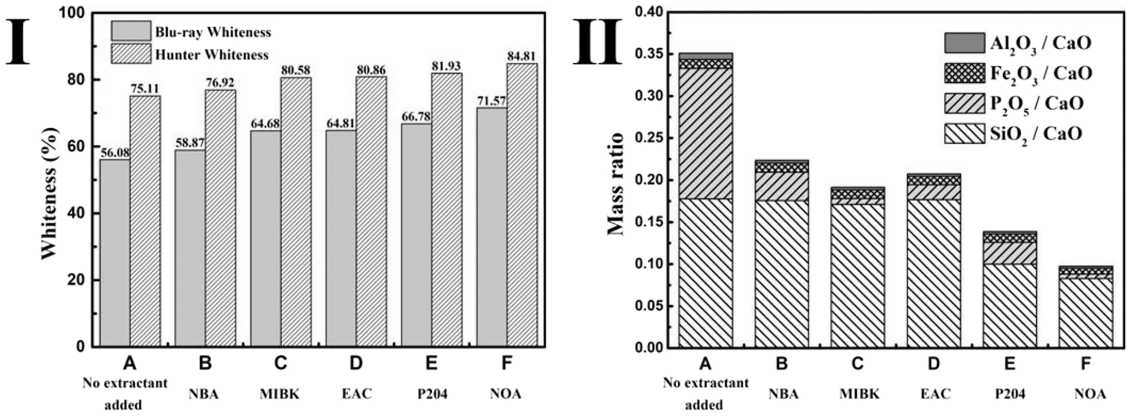

Figure 1. Comparison of (I) whiteness and (II) mass ratio of phosphogypsum treated with different extractants. (A) No extractant added, (B) N-butanol, (C) MIBK, (D) EAC, (E) P204, and (F) NOA.

the growth of calcium sulfate crystals and change the crystal size by adhering to the crystal edge during the growth of the calcium sulfate crystal.[12] Based on the investigation of the effects of impurities on the crystal growth of phosphogypsum, researchers also regulate the growth of calcium sulfate crystals by adding additives.[13,14] Different kinds of additives such as CTAB,[15] malic acid,[16] and so forth have been used to improve the crystal growth of calcium sulfate. Phosphate rock in China is almost medium-sized and low grade and has a high impurity content, which not only affects the crystallization of phosphogypsum and the conversion rate of phosphorus but also has a negative impact on the application performance of phosphogypsum.[17,18]

Therefore, the preparation of calcium sulfate crystals with uniform morphology and regular particle size distribution by regulating the crystal growth process of phosphogypsum plays an important role in improving the yield of phosphorus and promoting the resource utilization of phosphogypsum.[19−22] In our previous research, acid hydrolysis combined with impurity extraction has been used to remove the impurities in phosphogypsum post treatment process,[23] and purified gypsum has been prepared with high whiteness. Considering the characteristics of impurities dissolution in the WPA reaction process, a novel synergistic process of in situ impurities extraction and phophogypsum crystallization control in the WPA process has been put forward for the first time. Through the removal of impurities in the crystallization process, phosphogypsum may have uniform morphology and particle size, which is beneficial for the reduction of the P_2O_5 residual in phosphogypsum.

In this work, collaborative high-efficiency extraction of impurities and regulation of phosphogypsum crystallization in the acid hydrolysis process of WPA were carried out. Effects of *n*-octanol (NOA) addition as an extractant on the particle size, morphology, phase, and P_2O_5 content of phosphogypsum have been systematically investigated. The change of impurity occurrence forms in phosphogypsum caused by the addition of the extractant is also clarified. Through the research, theoretical basis can be provided for the novel innovative collaborative extraction process of WPA.

2. MATERIALS AND METHODS

2.1. Materials. Phosphate rock was provided by Chemical Group Co., Ltd. (Hubei, China), and the components are shown in Table 1. H_2SO_4 (Sinopharm Chemical Reagent Co., Ltd. ≥98 wt %), H_3PO_4 (Shanghai McLean Biochemical Technology Co., Ltd. ≥85 wt %), NOA (Shanghai McLean Biochemical Technology Co., Ltd. ≥99 wt %), and sulfonated kerosene (Jiangyin Wuyang hydrocarbon material technology Co., Ltd) were all of analytical grade. The experimental water was deionized water, and all chemical reagents were used without any further purification.

2.2. Experimental Procedure. Experiments were carried out in a 2 L round-bottom flask. In the actual production process, the returning acid predecomposed the phosphate rock, which further facilitated the reaction with H_2SO_4. The equations are as follows:

$$Ca_5F(PO_4)_3 + 7\,H_3PO_4 \rightarrow 5\,Ca(H_2PO_4)_2 + HF \quad (1)$$

$$Ca(H_2PO_4)_2\cdot H_2O + H_2SO_4 + nH_2O \rightarrow 2H_3PO_4 + CaSO_4\cdot nH_2O \quad (2)$$

The reflux acid was configured according to the mass fraction of H_3PO_4 of 35% and H_2SO_4 of 5%. Second, sulfuric acid was added into the reactor for acidolysis of phosphate rock, and the addition amount of sulfuric acid was determined according to the molar ratio of Ca/S of 1:1, Mg/S of 1:1, Al/S of 2:3, and Fe/S of 2:3. The additions of all raw materials were divided five times. Then, NOA and sulfonated kerosene were added with a certain dilution ratio and oil/aqueous (O/A) ratio into the reaction slurry. The reaction began when all raw materials were added. The reaction temperature was 80 °C, and the system was stirred with a flat-bladed stirrer at a constant rate of 200 rpm. When the reaction was finished, the slurry was allowed to stand, and the upper organic phase was poured out. Then, solid−liquid separation was carried out immediately. The filter cake was washed with deionized water of 80 °C, and the amount of washing water was 3 times of the filter cake.

https://doi.org/10.1021/acsomega.3c01168
ACS Omega 2023, 8, 28122−28132

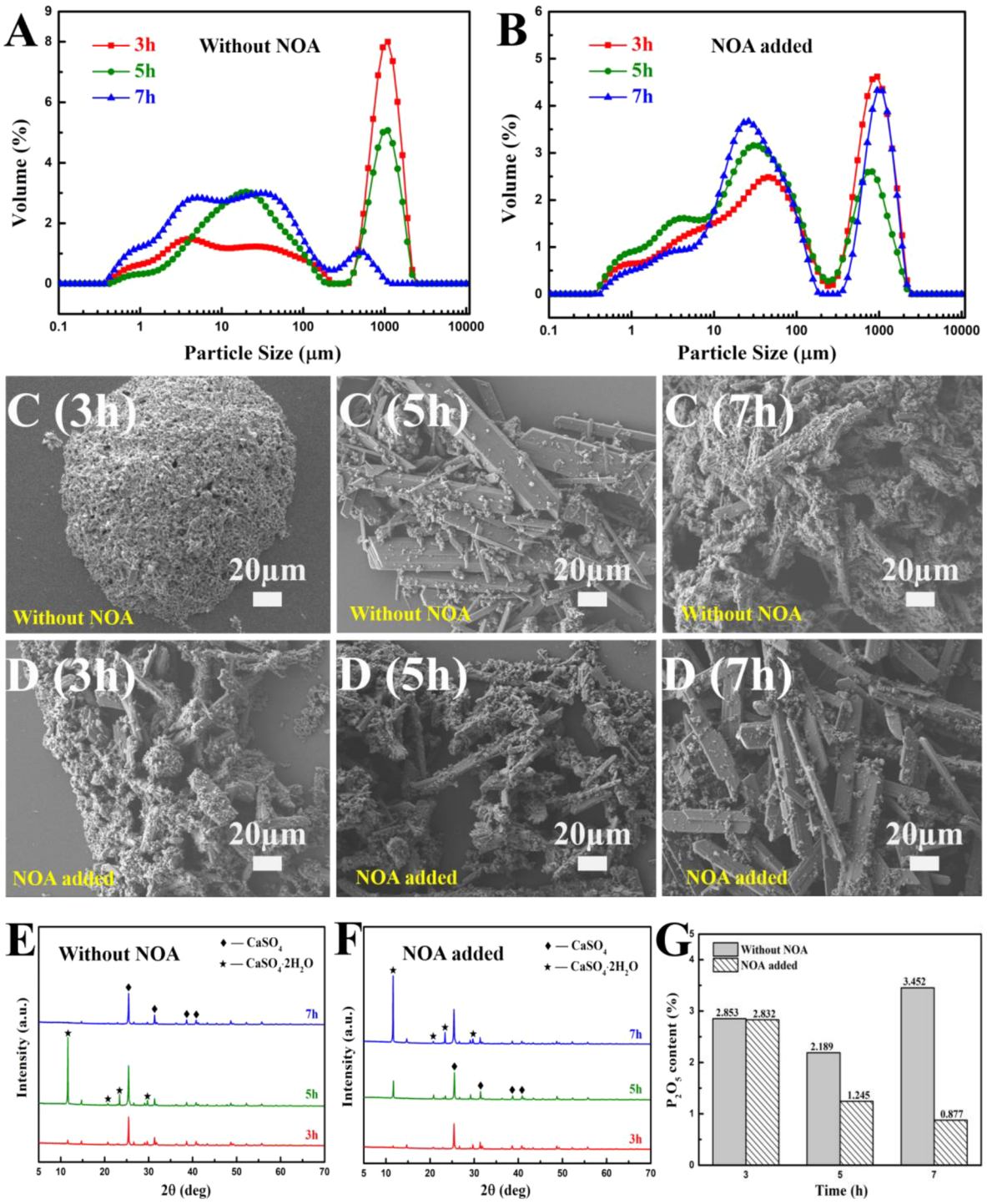

Figure 2. Effect of NOA addition on the reaction process and phosphogypsum crystallization at different reaction times. Particle size distribution of phosphogypsum (A) without NOA and (B) NOA added. Micrograph of phosphogypsum (C) without NOA and (D) NOA added. XRD phase composition spectrogram of phosphogypsum (E) without NOA and (F) NOA added. (G) Residual P_2O_5 content in phosphogypsum.

2.3. Analysis and Characterization. The particle size distribution of phosphogypsum was determined by a laser particle size analyzer (Mastersizer 2000 of Malvin Instrument Co., Ltd. in Britain). The composition of the phosphate rock and phosphogypsum samples was analyzed by an X-ray fluorescence spectrometer (PANalytical AXIOS,50 kV, 60 mA). X-ray diffraction (XRD, PANalytical B.V Empyrean, 40 mA, 40 kV, λ = 1.5406 Å, 5−70°) was used to analyze the crystal form under different experimental conditions. The micromorphology of phosphogypsum was observed by thermal field emission scanning electron microscopy (SEM, JSM-7610F). The main impurity elements in phosphogypsum were analyzed by X-ray photoelectron spectroscopy (XPS, ESCALAB 250Xi) using an Al Kα monochromated source (150 W, 20 eV pass energy, 650 μm spot size), and the binding energy of different elements was obtained. All binding energies were referenced to the C 1s peak at 284.8 eV of the surface adventitious carbon to correct the shift caused by the charge

https://doi.org/10.1021/acsomega.3c01168
ACS Omega 2023, 8, 28122−28132

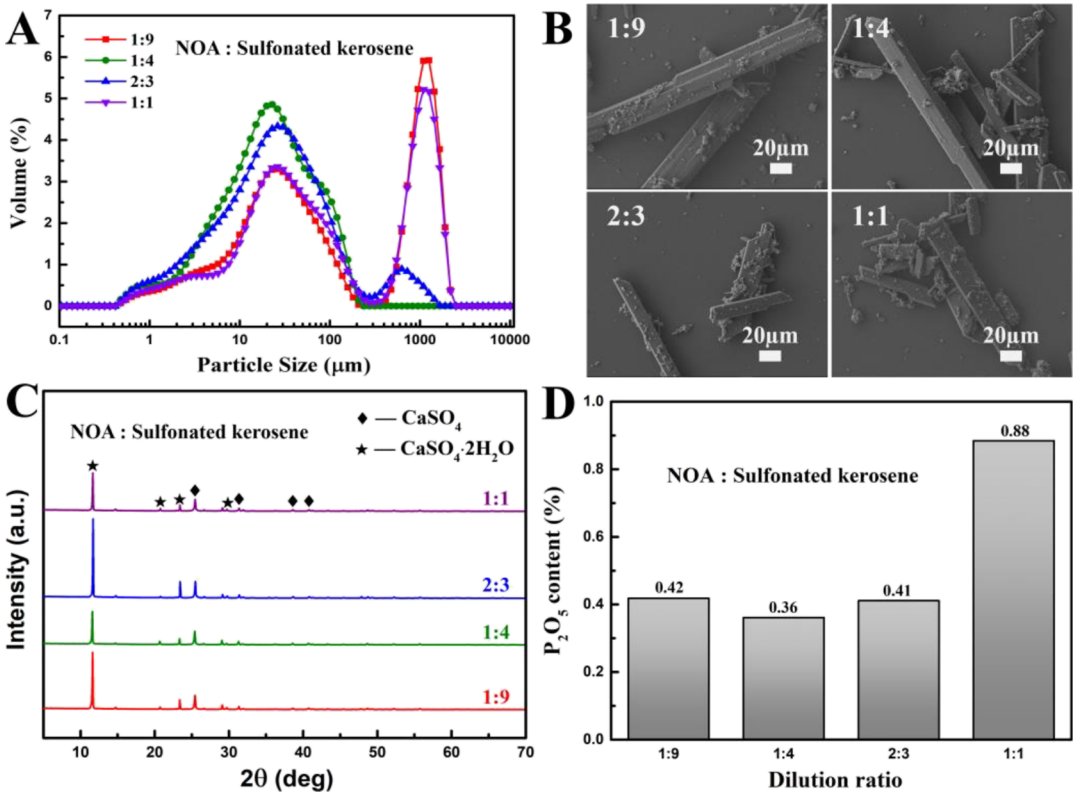

Figure 3. Phosphogypsum crystallization under different dilution ratios. (a) Particle size distribution, (b) SEM morphology, (c) XRD diffraction spectrum, and (d) variation of residual P_2O_5 content.

effect. The thermogravimetric curves of phosphogypsum samples were continuously recorded by a differential thermal/thermogravimetric synchronous analyzer (DTG-60H). The blue light whiteness and Hunter whiteness of phosphogypsum samples were tested by a whiteness meter (WSD-3C, Beijing Kangguang Optical Instrument Co., Ltd.).

3. RESULTS AND DISCUSSION

3.1. Investigation of Process Conditions. *3.1.1. Effect of Different Extractants.* In order to select a better extractant, the commonly used extractant in WPA was used to compare and analyze. The whiteness and impurities (Al, Fe, P, Si)/CaO mass ratio comparison of phosphogypsum under different extractant treatment conditions is shown in Figure 1. The blu-ray whiteness and Hunter whiteness of untreated phosphogypsum were only 56.08 and 75.11%. Adding organic substances such as N-butanol, methyl isobutyl ketone (MIBK), ethyl acetate (EAC), bis(2-ethylhexyl) phosphate (P204), and NOA can effectively improve the whiteness of phosphogypsum. Among them, the NOA extractant had the best treatment effect, which can improve the blu-ray whiteness and Hunter whiteness of phosphogypsum to 71.57 and 84.81%. Figure 1(II) shows that the impurities/CaO mass ratio of untreated phosphogypsum is 0.35. After adding the organic extractant, the impurities/CaO mass ratio of phosphogypsum was reduced. NOA treatment had the best effect, and the ratio could be reduced to about 0.10. Consequently, NOA extractant can effectively remove impurities in the phosphogypsum phase and improve its whiteness during WPA reaction.

3.1.2. Effect of NOA Addition. Compared with the original WPA, the effect of NOA addition on the crystallization process has been systematically investigated. The particle size distribution and morphology changes of phosphogypsum caused by the addition of NOA extractant at different reaction times are shown in Figure 2. While NOA was not added in the system, the particle size distribution of phosphogypsum was mainly 1000 μm particle agglomeration at 3 h. As the reaction time increased to 5 h, the agglomeration effect weakened, and the morphologies of phosphogypsum crystals were a mixture of short rod and long strip crystals with particle sizes of 20 and 1000 μm. The surface of some long strip crystals of calcium sulfate was relatively smooth. When the reaction time was further increased to 7 h, it could be found that the particle size of phosphogypsum was mainly 1−100 μm. There were many tiny particles on the surface of the phosphogypsum crystal, and the crystal surface became rough. It can be seen that the phase of phosphogypsum changed from anhydrite to dihydrate and then to anhydrite again. At the reaction time of 3 h, the diffraction peak of anhydrous calcium sulfate in phosphogypsum was strong and that of calcium sulfate dihydrate was weak. The morphology of phosphogypsum was mostly fine granular crystals, and the filtration rate was related to the average diameter of crystals.[24] The content of residual P_2O_5 in phosphogypsum was 2.853%. As the reaction time increased to 5 h, the diffraction peak of calcium sulfate dihydrate was strong, and the change of phosphogypsum morphology may be related to the phase leading to the formation of microanhydrite particles.[25] The increase of reaction time leads to the secondary nucleation of the crystal, and these particles may serve as a feedstock for gypsum crystal growth by a dissolution-reprecipitation mechanism.[26] As a consequence, the change of particle size and the generation of tiny particles increase the washing and filtration difficulties of phosphogypsum.[27]

https://doi.org/10.1021/acsomega.3c01168
ACS Omega 2023, 8, 28122−28132

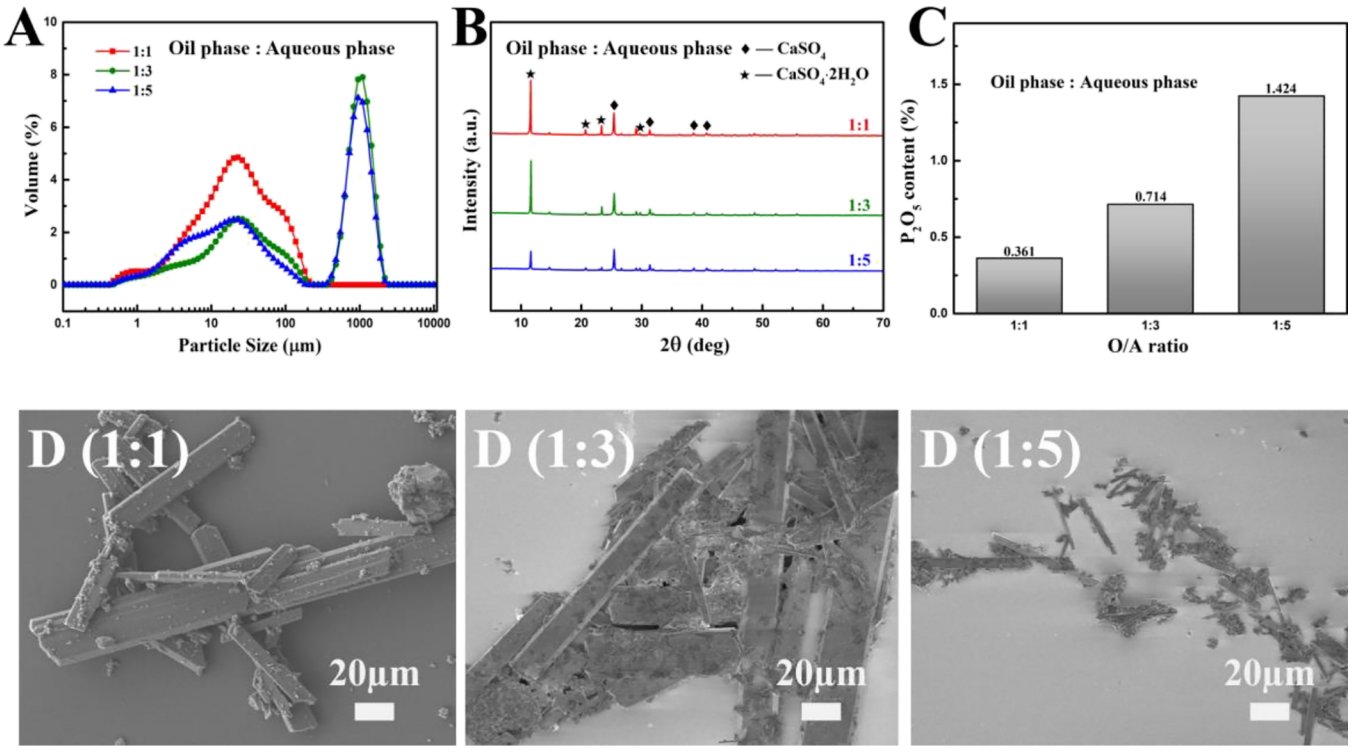

Figure 4. Phosphogypsum crystallization under different O/A ratios. (A) Particle size distribution, (B) XRD diffraction spectrum, (C) variation of residual P_2O_5 content, and (D) SEM morphology.

Residual P_2O_5 content in phosphogypsum increased from 2.189 to 3.452% with the increase of reaction time from 5 to 7 h.

Under the condition of adding NOA, the particle size of phosphogypsum was distributed in the range of 20−40 μm and 900 μm. According to the morphology of phosphogypsum, the size of calcium sulfate crystals gradually increased, and the surface of the crystals also changed from rough to smooth with the prolongation of the reaction time. Small particles attached on the long strip of calcium sulfate crystals were significantly less, and the calcium sulfate crystals show a relatively uniform flake crystal effect. Meanwhile, the addition of NOA also slowed down the phase change of phosphogypsum. It can be found that the main phase of phosphogypsum obtained under the condition of adding extractant NOA was composed of dihydrate and anhydrite, and the content of the both in phosphogypsum changed with the change of reaction time. With the increase of reaction time, the diffraction peak of calcium sulfate dihydrate gradually increased. When the reaction time reached 7 h, the phosphogypsum phase was mainly calcium sulfate dihydrate. At the same time, the content of residual P_2O_5 in phosphogypsum gradually decreased with the increase of growth and smoothness of the particles. The residual P_2O_5 content in phosphogypsum was as low as 0.877% at 7 h. Compared with the result without NOA addition, the uniform and coarse calcium sulfate dihydrate crystals improve the washing efficiency and low down residual P_2O_5 content in phosphogypsum.

3.1.3. Effect of the Dilution Ratio. The viscosity of NOA is as high as 8.93 mPa s at 298.2 K, which limits the fluidity and the mass transfer velocity. To improve the hydrodynamics of the extraction, diluents of low density and viscosity and which are miscible with the extractant were used. Because aliphatic diluents provided higher extraction efficiencies,[28] sulfonated kerosene was selected as the diluent. Sulfonated kerosene contains alkane and a small proportion of aromatic hydrocarbon. It is commonly used as a nonpolar diluent in various extraction processes. Another reason for choosing sulfonated kerosene as the diluent was that the reaction acid of WPA process is sulfuric acid, and sulfonated kerosene has good stability in this system (Figure 3).

It can be seen that the particle size distribution of phosphogypsum crystals can be divided into two peaks:large particles with the size around 1000 μm and small particles with the size 30 μm when the ratio of NOA:sulfonated kerosene was 1:9. When the dilution ratio was 1:4, the particle size of the calcium sulfate crystal presented a homogeneous distribution, and the main size of the crystal was around 25 μm. However, the surface of the rod was very smooth according to the morphologies of phosphogypsum. When the dilution ratio changed to 2:3, the peak of the large particle size at around 1000 μm appeared again, but the proportion was relatively low. Particle size distribution of phosphogypsum crystals of the dilution ratio of 1:1 was very similar to that of the dilution ratio of 1:9. The peak at around 1000 μm was significant, and the morphology of the crystals was long strip and a small amount of short rod.

The phase change with the dilution ratio has also been investigated. It can be seen that the main phases of phosphogypsum were calcium sulfate dihydrate. The influence of dilution ratios on the phase was little, but the residual P_2O_5 content in phosphogypsum changed with the increase of dilution ratio. When the dilution ratio of NOA:sulfonated kerosene was 1:9, the content of residual P_2O_5 in phosphogypsum was 0.418%. When the dilution ratio was increased to 1:4, the residual P_2O_5 content in phosphogypsum decreased to 0.361%. With the increase of the dilution ratio and the decrease of NOA addition, the residual P_2O_5 content

https://doi.org/10.1021/acsomega.3c01168
ACS Omega 2023, 8, 28122−28132

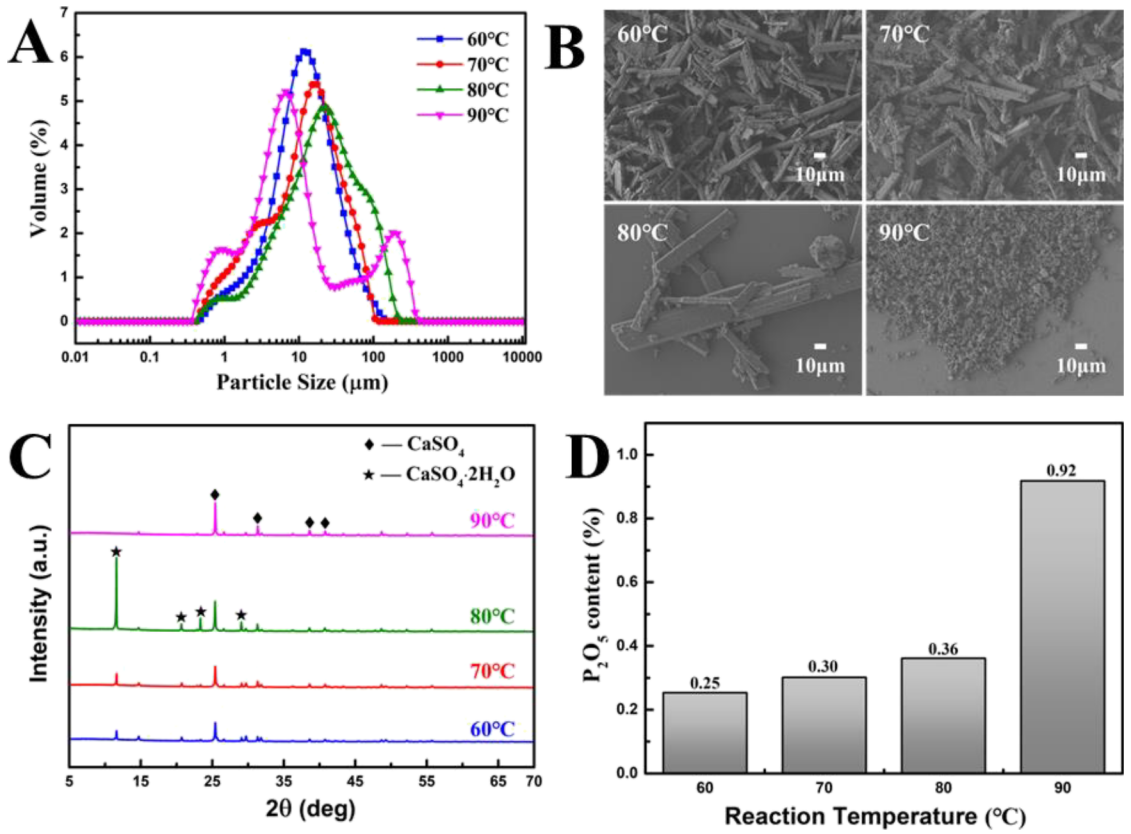

Figure 5. Phosphogypsum crystallization under different reaction temperatures. (A) Particle size distribution, (B) SEM morphology, (C) XRD diffraction spectrum, and (D) variation of residual P_2O_5 content.

in phosphogypsum increased. When the dilution ratio of NOA:sulfonated kerosene was 1:1, the P_2O_5 content in phosphogypsum increased to 0.884%. In conclusion, it can be seen that under the condition of dilution ratio of 1:4, the obtained phosphogypsum was uniform and coarse calcium sulfate dihydrate crystal, and the content of residual P_2O_5 in phosphogypsum was as low as 0.361%.

3.1.4. Effect of the O/A Ratio. Phosphogypsum with a low content of P_2O_5 and good crystal morphology were obtained in the ratio of NOA:sulfonated kerosene at 1:4. Effect of the change of organic phase content on the crystal growth of phosphogypsum was further investigated as shown in Figure 4. It can be found that when the O/A ratio was 1:1, the calcium sulfate crystal grew evenly, the particle size of calcium sulfate presented a normal distribution, and the main crystal size was about 25 μm. Diffraction peak strength of calcium sulfate dihydrate was relatively high, and the residual P_2O_5 content in phosphogypsum was 0.361%. When the O/A ratio changed to 1:3, the peak at around 1000 μm appeared, and the main phase was calcium sulfate dihydrate. However, the crystals of phosphogypsum did not grow well, and there were many small short rod crystals around the long strip crystals of calcium sulfate with a rough surface. The increase of particle size may be caused by the aggregation of small particles, which lead to the washing difficulty and increase of residual P_2O_5 content. Residual content of P_2O_5 in phosphogypsum was 0.714%. When the O/A ratio changed to 1:5, the morphology of the calcium sulfate crystal was mainly fine rod-shaped, and there was no long strip-shaped massive crystal. The proportion of anhydrous calcium sulfate in phosphogypsum grew, and the content of residual P_2O_5 in phosphogypsum reached 1.424%. According to the optimization of dilution ratio and O/A ratio, 0.412 kg of NOA and 1.594 kg of sulfonated kerosene may be used to treat 1 kg of phosphate rock. However, the extractant can be reused after the treatment, and the loss amount has been discussed in the following sections.

3.1.5. Effect of the Reaction Temperature. On the basis of the reaction time of 7 h, the dilution ratio of NOA to sulfonated kerosene of 1:4, and the O/A ratio of organic phase to acid solution of 1:1, the effects of different temperatures were studied as shown in Figure 5. When the reaction system was at a low temperature of 60 °C, the particle size of phosphogypsum was mainly distributed at 10 μm, and the morphology of calcium sulfate was mostly short blocky crystals, with short rod-shaped and granular fine particles in between. When the reaction temperature rose to 70 °C, the particle size of phosphogypsum increased to 11 μm, but the fine particles on the surface of calcium sulfate crystal increased, most of which were small calcium sulfate particles of 1−2 μm. When the reaction temperature reached 80 °C, the particle size of phosphogypsum was distributed at 12 and 100 μm, and it can be found that the calcium sulfate crystal was relatively uniform and the fine particles attached to the surface of the larger crystal were reduced by combining with the micro-topography. When the temperature rose to 90 °C, the main particle size of phosphogypsum decreased to 7 μm, and the morphology was mainly fine calcium sulfate particles. According to the particle size distribution, the particle size distribution of 110 μm was mainly due to the agglomeration of fine calcium sulfate particles.

Second, the phase transformation of phosphogypsum and the change rule of residual P_2O_5 at different temperatures were

https://doi.org/10.1021/acsomega.3c01168
ACS Omega 2023, 8, 28122−28132

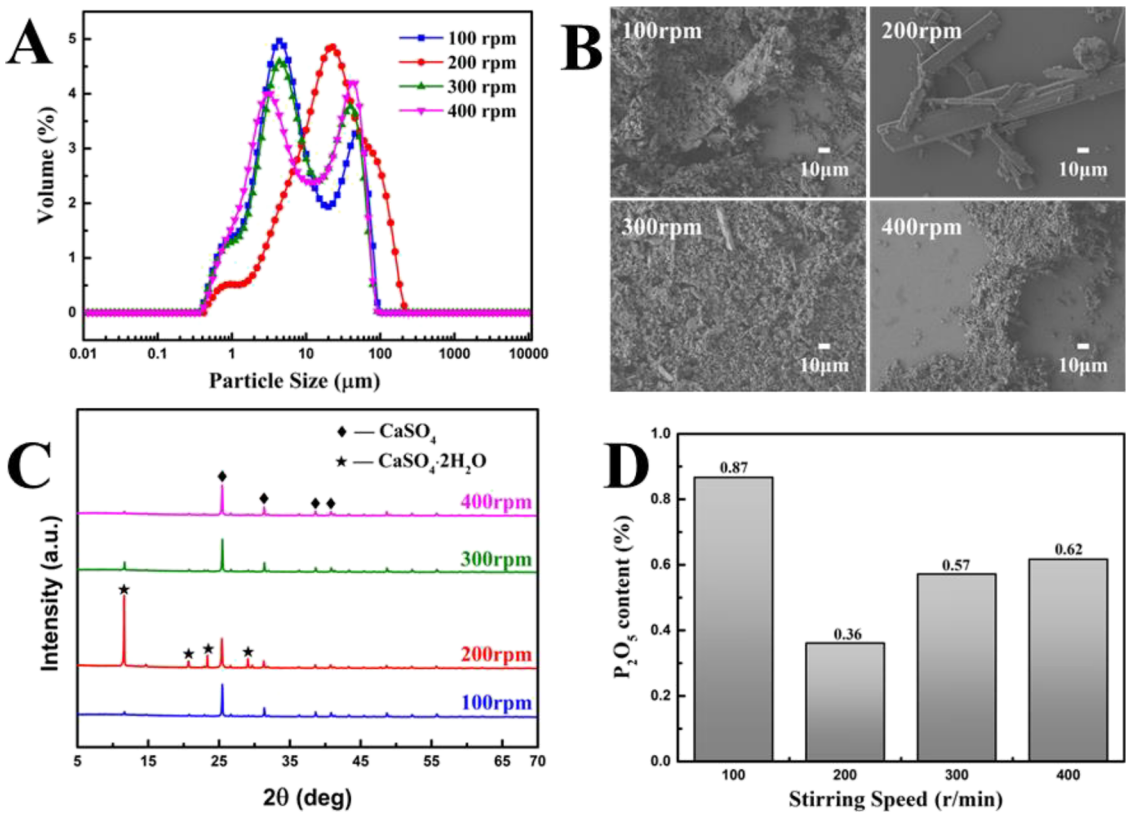

Figure 6. Phosphogypsum crystallization under different stirring speeds. (A) Particle size distribution, (B) SEM morphology, (C) XRD diffraction spectrum, and (D) variation of residual P_2O_5 content.

analyzed, When the reaction temperature was 60 °C, the phase of phosphogypsum was mainly anhydrous calcium sulfate, accompanied by a small amount of calcium sulfate dihydrate, and the residual P_2O_5 content in phosphogypsum was 0.25%. With the increase of reaction temperature, the main phase of phosphogypsum changed. At the temperature of 60−80 °C, the main phase of phosphogypsum changed from anhydrous calcium sulfate to dihydrate calcium sulfate. When the reaction temperature reached 80 °C, the main phase of phosphogypsum was dihydrate calcium sulfate, and the content of residual P_2O_5 increased slightly to 0.36%. When the temperature was further raised to 90 °C, the phase of calcium sulfate dihydrate in phosphogypsum disappeared, and the phosphogypsum was mainly composed of anhydrous calcium sulfate, which was consistent with the crystal morphology of fine particles. As a result, the washing performance of the filter cake decreased,[7] and the residual P_2O_5 content in phosphogypsum increased to 0.92%. The change rule of the phosphogypsum phase with temperature is in accordance with the phase diagram[29] of the $CaSO_4$ crystal, phosphoric acid concentration, and temperature. Based on the above analysis, when the temperature was 80 °C, phosphogypsum was dominated by calcium sulfate dihydrate, with the largest crystal size and regular morphology. The content of residual P_2O_5 was relatively low, and the reaction temperature was comprehensively recommended as 80 °C.

3.1.6. Effect of Stirring Speeds. The influence of different stirring speeds on the particle size, morphology, phase, and P_2O_5 content of phosphogypsum is shown in Figure 6. Compared with the stirring speed of 200 r/min, too high or too low stirring speed led to double peaks in the particle size distribution of phosphogypsum. When the stirring speed was 100 r/min, the particle sizes of phosphogypsum were both 4 and 40 μm. At this time, the morphology of phosphogypsum coexisted with long strip crystals and fine granular crystals. Due to the low stirring speed, most fine calcium sulfate particles were attached and wrapped around the strip crystals. When the stirring speed increased to 200 r/min, calcium sulfate presented uniform strip crystals, the main particle sizes of phosphogypsum were distributed at 12 and 100 μm, and the crystal surfaces with larger particle sizes did not appear to be wrapped. However, when the stirring speed was increased to 300 r/min or 400 r/min, the phosphogypsum crystals could not grow completely under the action of strong mechanical stirring. The morphology of phosphogypsum was mainly fine and messy granular crystals of calcium sulfate, with local agglomeration. The particle size of phosphogypsum appeared in the form of small crystals of 13 μm and large aggregates of about 80 μm.

As different stirring speeds will lead to different crystal appearances,[30,31] the change of phase and the residual P_2O_5 content of phosphogypsum at different stirring speeds were explored. Compared with the stirring speed of 200 r/min, the phase of phosphogypsum obtained at lower or higher stirring speed was mainly anhydrous calcium sulfate, accompanied by a small amount of calcium sulfate dihydrate, and the content of residual P_2O_5 in phosphogypsum decreased first and then increased with the increase of stirring speed. At the stirring speeds of 100, 300, and 400 r/min, the residual P_2O_5 content in phosphogypsum was 0.87, 0.57, and 0.62%, respectively. When the stirring speed was kept at 200 r/min, the obtained phosphogypsum was mainly composed of calcium sulfate dihydrate, and the residual P_2O_5 content of phosphogypsum was as low as 0.36%.

https://doi.org/10.1021/acsomega.3c01168
ACS Omega 2023, 8, 28122−28132

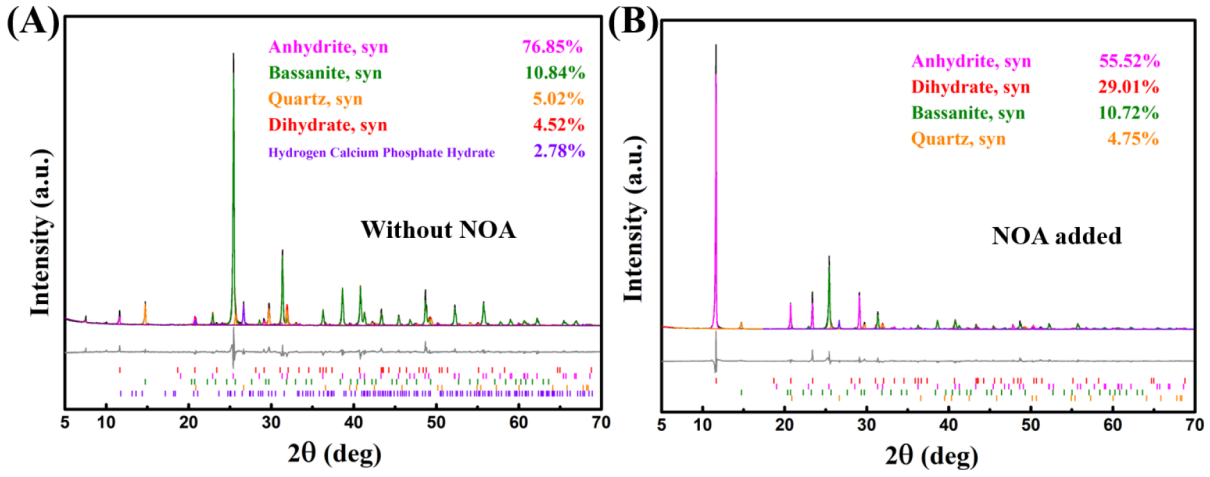

Figure 7. XRD Rietveld quantitative analysis diagram of phosphogypsum (A) without extractant and (B) with extractant.

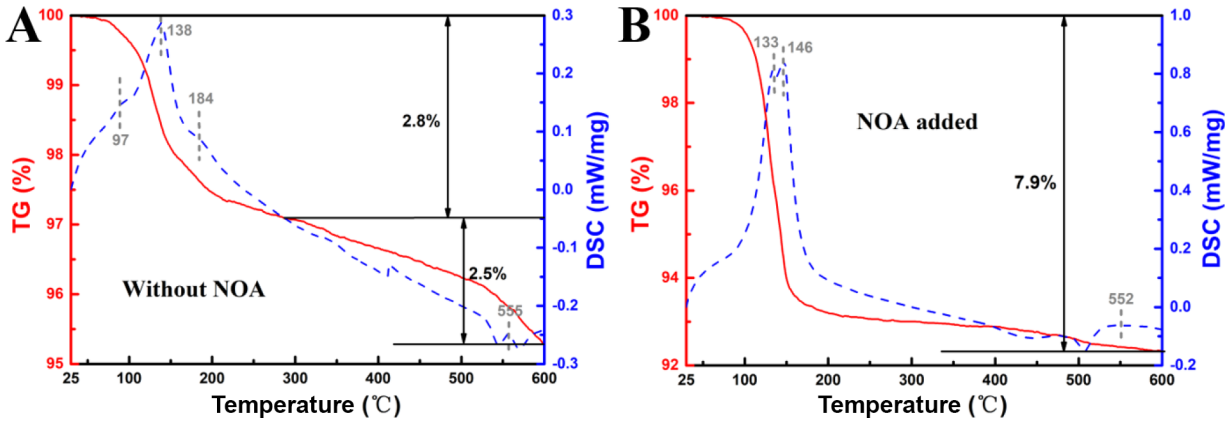

Figure 8. TG-DSC diagram of phosphogypsum (A) with the extractant and (B) without the extractant.

In conclusion, based on the above analysis of effects of process conditions, the reaction time, the dilution ratio, the O/A ratio, the reaction temperature, and stirring speeds are synthetically regarded as 7 h 1:4, 1:1, 80 °C and 200 r/min, respectively. Under optimized conditions, calcium sulfate presented uniform strip crystals, the main particle sizes of phosphogypsum were distributed at 12 and 100 μm, and the crystal surfaces with larger particle sizes did not appear to be wrapped. Meanwhile, the content of P_2O_5 in phosphogypsum could be reduced to 0.36%, and the impurities content met the China national standard *Treatment and disposal specification for phosphogypsum* (GB/T 32124-2015).

3.2. Effect of NOA Addition on Phosphogypsum. *3.2.1. Phase and Thermal Stability Comparison.* The phosphogypsum obtained at optimized conditions with NOA extractant has been analyzed and compared with that obtained without NOA extractant. First, XRD Rietveld quantitative analysis has been done to investigate the effect on the phase of phosphogypsum, and the results can be seen in Figure 7.

It can be found that the content of phosphogypsum with NOA extractant addition was mainly $CaSO_4$. The content of anhydrite and dihydrate gypsum was 76.85 and 4.52%, respectively. Meanwhile, there also exists little amount of bassanite (10.84%) and quartz (5.08%). When the NOA extractant was added into the system, the change of phosphogypsum phase from dihydrate to anhydrite was slowed down. The main phase in phosphogypsum was also anhydrite, but the content decreased to 55.52% and the content of dehydrate increased to 29.01%. The content of bassanite and quartz remained nearly the same.

The phase change can also be reflected through thermal analysis, which can be seen in Figure 8. When phosphogypsum was heated from 90 to 200 °C, the weight loss of phosphogypsum was 2.8% without NOA extractant. In this temperature range, the mass loss may be caused by the free water volatilization and phase change of phosphogypsum.[32] According to the ratio of crystallization water in gypsum and the phase analysis results in Figure 8, the weight loss contained the crystallization (2.2%) and free water (0.6%) volatilization in the phosphogypsum. When the temperature reached 600 °C, the mass loss of phosphogypsum was about 2.8%. This may be caused by the carbon volatilization, which existed in the phosphate rock and mixed into phosphogypsum in the acidolysis process. Meanwhile, decomposition of $CaSO_4$ may also occur to release SO_2.[33−35] When NOA extractant was added, the phase content of dehydrate increased. Therefore, the mass loss was higher in the range of 90−200 °C compared with that without NOA addition. According to the results of XRD Rietveld quantitative analysis, the content of crystallization and free water in phosphogypsum was 6.74 and 0.6%, respectively. Under this situation, NOA extractant and sulfonated kerosene are unavoidably entrained in phosphogypsum. The boiling point of extractant was 198 °C. However, the mass loss over 200 °C is only 0.56%, which is much lower

https://doi.org/10.1021/acsomega.3c01168
ACS Omega 2023, 8, 28122−28132

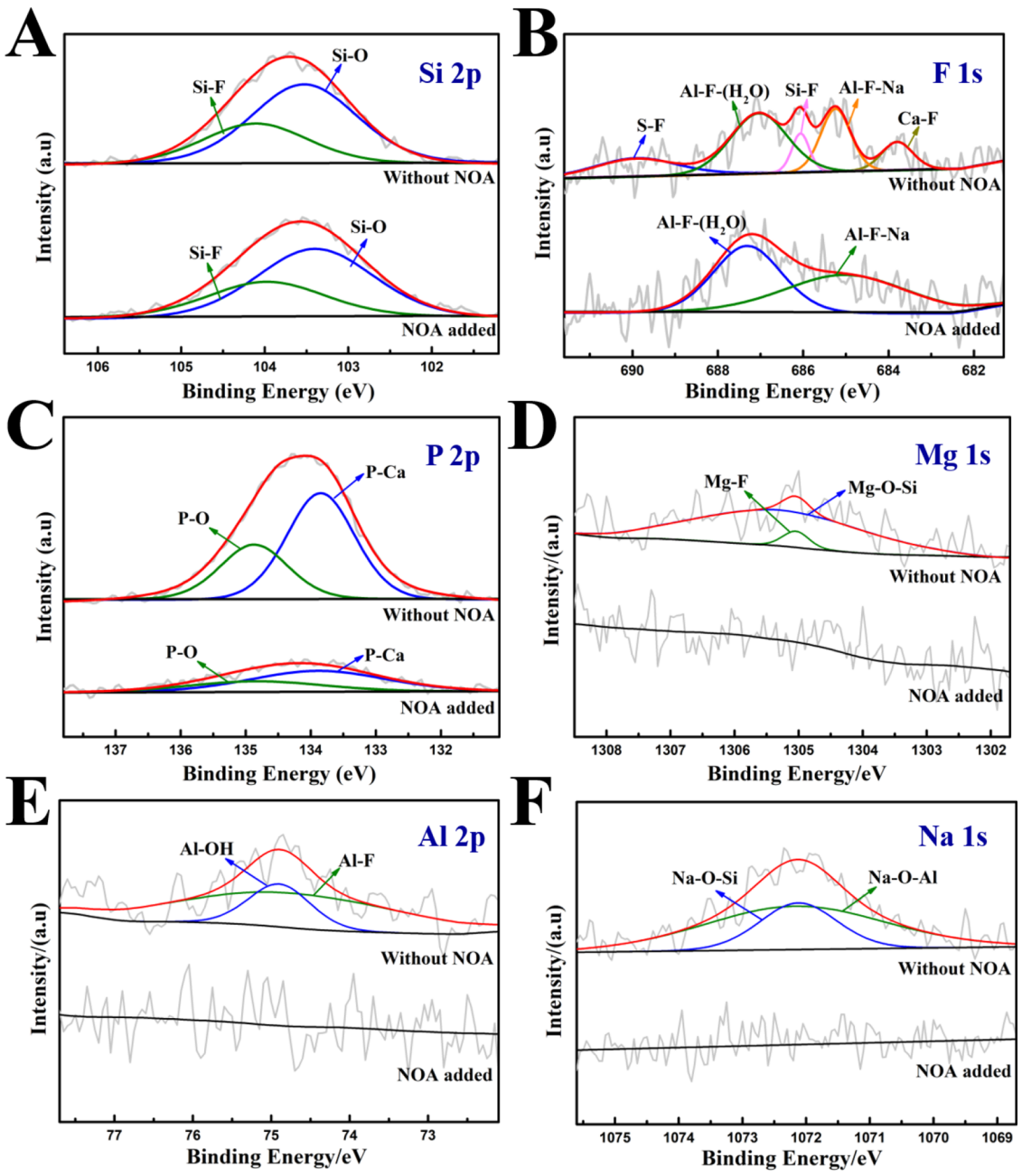

Figure 9. XPS diagram of phosphogypsum with NOA added or not. (A) Si 2p scan spectra; (B) F 1s scan spectra; (C) P 2p scan spectra; (D) Mg 1s scan spectra; (E) Al 2p scan spectra; (F) Na 1s scan spectra.

than that without NOA. The mass loss contains the volatilization of the extractant and the impurities. It meant the impurities removal effect by NOA through the interaction between oil phase and carbon[36] and the entrainment of extractant in phosphogypsum is less.

3.2.2. Impurities Amount and Occurrence in Phosphogypsum. Through the investigation process of NOA extractant, it can be seen that the phase, mass loss, and entrained P_2O_5 can be largely affected. Meanwhile, the impurities affect the crystal size and morphology in the crystallization process, which depends on the growth rate of different crystal faces.[15,37] To investigate the effect of NOA addition on the impurity components and occurrence in phosphogypsum, XPS analysis was done, and the results are shown in Figure 9. It can be found that P mainly existed in the form of insoluble calcium fluorophosphates such as $Ca_5(PO_4)_3$ and $Ca_{10}(PO_4)_6F_2$. The addition of NOA caused the decrease of entrained P_2O_5 amount, and it led to the intensity reduction of the peaks related to the P element. The Si 2p spectrum of phosphogypsum obtained without NOA can be effectually fitted with two peaks at 687.72 and 350.85 eV, which represented the existence of the Si−O group structure in silica (SiO_2)[38] and the Si−F group structure in fluorosilicates (Na_2SiF_6).[39] The amounts counted for 66.23 and 33.77%, respectively. The addition of NOA had no obviously effect on the residual of Si. The spectrum of phosphogypsum under this situation was similar to the above, and the amounts for two fitting peaks were 65.79 and 34.21%, respectively.

Peaks of Na, Mg, and Al may also appear in the XPS survey spectra of phosphogypsum obtained without NOA extractant.

https://doi.org/10.1021/acsomega.3c01168
ACS Omega 2023, 8, 28122−28132

Na mainly existed as sodium salt and forms aluminate (1072.17 eV) and silicate (1072.12 eV). Mg existed in the formation of magnesium silicate (1305.29 eV). Meanwhile, the substitution of Mg on Ca can form MgF_2 (1305.04 eV). Al mainly existed in the form of fluoride or aluminum fluoride with crystal water. The existence of F in phosphogypsum is very complicated, and the signal can be divided into five peak shapes. They represent the combination of S−F (689.92 eV), Al−F (687.03 eV), Si−F (686.06 eV), Al−F−Na (685.24 eV), and Ca−F (683.80 eV). Combined with the analysis of other impurities, the main forms of F in phosphogypsum were fluosilicate (Na_2SiF_6), aluminum fluoride with crystal water ($AlF_3{\cdot}3H_2O$), fluoroaluminate (Na_3AlF_6), and insoluble $Ca_{10}(PO_4)_6F_2$.[39] When NOA extractant was added and the spectrum had no obvious characteristic peak for Na, Mg and Al impurities, it meant that the contents of such impurities were very low. Fitting peaks of F also decreased. At the same time, F only existed in residual crystal water aluminum fluoride ($AlF_3{\cdot}3H_2O$) and a small amount of fluoroaluminate (Na_3AlF_6). It meant that the addition of NOA extractant can effectively transform the impurities from phosphogypsum and reduce the residual Na, Mg, Al, F, and other impurities in phosphogypsum.[40−42]

In conclusion, the addition of NOA extractant can effectively reduce the residual Na, Mg, Al, F, and other impurities in phosphogypsum. The main impurity forms of phosphogypsum after acid hydrolysis and NOA extraction are silicate, aluminum fluoride with crystal water, aluminate, phosphate, and fluoride.

4. CONCLUSIONS

Based on the novel process of phosphogypsum acidolysis with synergistic extraction, the high-efficiency removal of impurities and the crystallization control of phosphogypsum during the acidolysis of WPA were studied. The results show that under the optimum process conditions of reaction time 7 h, dilution ratio 1:4, O/A ratio 1:1, stirring speed 200 rpm, and reaction temperature 80 °C, phosphogypsum presented uniform strip crystals. The main particle sizes were distributed at 12 and 100 μm, and the content of P_2O_5 could be reduced to 0.36%. Besides, the results of XRD Rietveld quantitative and TG-DSC showed that the addition of NOA promoted the crystallization of calcium sulfate dihydrate in phosphogypsum, and the loss of NOA was less. XPS showed that NOA extractant can effectively reduce the residual Na, Mg, Al, F, and other impurities in phosphogypsum, which promoted the growth of phosphogypsum to form uniform long strip crystals, and the main impurities of phosphogypsum after acid hydrolysis and extraction were silicate, crystal water aluminum fluoride, and aluminate. The results can provide a reference for impurity removal from wet-process phosphoric acid source and phosphogypsum crystallization control.

AUTHOR INFORMATION

Corresponding Author

Huiquan Li − *CAS Key Laboratory of Green Process and Engineering, National Engineering Research Center of Strategic Metal Resources Green Recycling and Utilization, Institute of Process Engineering, Chinese Academy of Sciences, Beijing 100190, China; School of Chemical Engineering, University of Chinese Academy of Sciences, Beijing 100049, China;* orcid.org/0000-0002-3702-3164; Phone: +86-10-82544830; Email: hqli@ipe.ac.cn

Authors

Ganyu Zhu − *CAS Key Laboratory of Green Process and Engineering, National Engineering Research Center of Strategic Metal Resources Green Recycling and Utilization, Institute of Process Engineering, Chinese Academy of Sciences, Beijing 100190, China*

Yunrui Yang − *CAS Key Laboratory of Green Process and Engineering, National Engineering Research Center of Strategic Metal Resources Green Recycling and Utilization, Institute of Process Engineering, Chinese Academy of Sciences, Beijing 100190, China; School of Chemical Engineering, University of Chinese Academy of Sciences, Beijing 100049, China*

Lei He − *Yidu Xingfa Chemical Co. LTD, Yidu, Hubei 443311, China*

Ziheng Meng − *CAS Key Laboratory of Green Process and Engineering, National Engineering Research Center of Strategic Metal Resources Green Recycling and Utilization, Institute of Process Engineering, Chinese Academy of Sciences, Beijing 100190, China*

Guangming Zheng − *Yidu Xingfa Chemical Co. LTD, Yidu, Hubei 443311, China*

Fang Li − *Yidu Xingfa Chemical Co. LTD, Yidu, Hubei 443311, China*

Xiaodan Su − *School of Chemistry and Chemical Engineering, University of Jinan, Jinan 250022, China*

Benjun Xi − *Hubei Three Gorges Laboratory, Yichang, Hubei 443311, China*

Zhongjun Li − *Hubei Three Gorges Laboratory, Yichang, Hubei 443311, China*

Complete contact information is available at: https://pubs.acs.org/10.1021/acsomega.3c01168

Notes

The authors declare no competing financial interest.

ACKNOWLEDGMENTS

The work was supported by the National Key R&D Program of China (no. 2022YFC3902701), the National Natural Science Foundation of China (no. 22078344), and the Hubei Three Gorges Laboratory (no. SC211015, SC211001).

REFERENCES

(1) Ashley, K.; Cordell, D.; Mavinic, D. A Brief History of Phosphorus: From the Philosopher's Stone to Nutrient Recovery and Reuse. *Chemosphere* **2011**, *84*, 737−746.

(2) Li, J. Y.; Qian, Y. M.; Wang, L.; He, X. M. Nitrogen-Doped Carbon for Red Phosphorous Based Anode Materials for Lithium Ion Batteries. *Materials* **2018**, *11*, 134.

(3) El-Didamony, H.; Gado, H. S.; Awwad, N. S.; Fawzy, M. M.; Attallah, M. F. Treatment of Phosphogypsum Waste Produced from Phosphate Ore Processing. *J. Hazard. Mater.* **2013**, *244-245*, 596−602.

(4) Zhou, J.; Gao, H.; Shu, Z.; Wang, Y. X.; Yan, C. J. Utilization of Waste Phosphogypsum to Prepare Non-Fired Bricks by A Novel Hydration-Recrystallization Process. *Constr. Build. Mater.* **2012**, *34*, 114−119.

(5) Zhang, L.; Wang, B. M.; Ying, D. Y.; Liu, Y.; Hua, Q. X.; Liu, L.; Tang, J. W. Effect of the Impurity Ions on the Crystallization of Urea Phosphate. *Int. J. Chem. React. Eng.* **2019**, *17*, No. 20180275.

(6) Li, J.; Wang, J. H.; Zhang, Y. X. Effects of the Impurities on the Habit of Gypsum in Wet-Process Phosphoric Acid. *Ind. Eng. Chem. Res.* **1997**, *36*, 2657−2661.

(7) Kruger, A.; Focke, W. W.; Kwela, Z.; Fowles, R. Effect of Ionic Impurities on the Crystallization of Gypsum in Wet-Process Phosphoric Acid. *Ind. Eng. Chem. Res.* **2001**, *40*, 1364−1369.
(8) Mao, X. L.; Song, X. F.; Lu, G. M.; Sun, Y. Z.; Xu, Y. X.; Yu, J. G. Effects of Metal Ions on Crystal Morphology and Size of Calcium Sulfate Whiskers in Aqueous HCl Solutions. *Ind. Eng. Chem. Res.* **2014**, *53*, 17625−17635.
(9) Yang, L. C.; Wu, Z. B.; Guan, B. H.; Fu, H. L.; Ye, Q. Q. Growth Rate of α-Calcium Sulfate Hemihydrate in K-Ca-Mg-Cl-H_2O Systems at Elevated Temperature. *J. Cryst. Growth* **2009**, *311*, 4518−4524.
(10) Hamdona, S. K.; Al Hadad, U. A. Crystallization of Calcium Sulfate Dihydrate in the Presence of Some Metal Ions. *J. Cryst. Growth* **2007**, *299*, 146−151.
(11) Ahmed, S. B.; Tlili, M. M.; Amami, M.; Amor, M. B. Gypsum Precipitation Kinetics and Solubility in the NaCl-$MgCl_2$-$CaSO_4$-H_2O System. *Ind. Eng. Chem. Res.* **2014**, *53*, 9554−9560.
(12) Hasson, D.; Addai-Mensah, J.; Metcalfe, J. Filterability of Gypsum Crystallized in Phosphoric Acid Solution in the Presence of Ionic Impurities. *Ind. Eng. Chem. Res.* **1990**, *29*, 867−875.
(13) Jiang, W. G.; Pan, H. H.; Tao, J. H.; Xu, X. R.; Tang, R. K. Dual Roles of Borax in Kinetics of Calcium Sulfate Dihydrate Formation. *Langmuir* **2007**, *23*, 5070−5076.
(14) Prisciandaro, M.; Olivieri, E.; Lancia, A.; Musmarra, D. PBTC as an Antiscalant for Gypsum Precipitation: Interfacial Tension and Activation Energy Estimation. *Ind. Eng. Chem. Res.* **2012**, *51*, 12844−12851.
(15) Feldmann, T.; Demopoulos, G. P. Effects of Crystal Habit Modifiers on the Morphology of Calcium Sulfate Dihydrate Grown in Strong $CaCl_2$-HCl Solutions. *J. Chem. Technol. Biotechnol.* **2014**, *89*, 1523−1533.
(16) Guan, Q. J.; Hu, Y. H.; Tang, H. H.; Sun, W.; Gao, Z. Y. Preparation of α-$CaSO_4$.$(1/2)H_2O$ with Tunable Morphology from Flue Gas Desulphurization Gypsum Using Malic Acid as Modifier: A Theoretical and Experimental Study. *J. Colloid Interface Sci.* **2018**, *530*, 292−301.
(17) Li, B.; Shu, J. C.; Yang, L.; Tao, C. Y.; Chen, M. J.; Liu, Z. H.; Liu, R. L. An innovative method for simultaneous stabilization/solidification of PO43- and F- from phosphogypsum using phosphorus ore flotation tailings. *J. Cleaner Prod.* **2019**, *235*, 308−316.
(18) Singh, M.; Garg, M.; Verma, C. L.; Handa, S. K.; Kumar, R. An improved process for the purification of phosphogypsum. *Constr. Build. Mater.* **1996**, *10*, 597−600.
(19) Yang, L.; Cao, J. X.; Luo, T. Effect of Mg^{2+}, Al^{3+}, and Fe^{3+} Ions on Crystallization of Type α Hemi-Hydrated Calcium Sulfate Under Simulated Conditions of Hemi-Hydrate Process of Phosphoric Acid. *J. Cryst. Growth* **2018**, *486*, 30−37.
(20) El-Shall, H.; Rashad, M. M.; Abdel-Aal, E. A. Effect of Phosphonate Additive on Crystallization of Gypsum in Phosphoric and Sulfuric Acid Medium. *Cryst. Res. Technol.* **2002**, *37*, 1264−1273.
(21) Gayevskii, V. R.; Kochmarskii, V. Z.; Gayevska, S. G. Nucleation and Crystal Growth of Calcium Sulfate Dihydrate From Aqueous Solutions: Speciation of Solution Components, Kinetics of Growth, and Interfacial Tension. *J. Cryst. Growth* **2020**, *548*, No. 125844.
(22) Doğan, Ö.; Akyol, E.; Öner, M. Polyelectrolytes inhibition effect on crystallization of gypsum. *Cryst. Res. Technol.* **2004**, *39*, 1108−1114.
(23) Zhao, H. T. *Fundamental Study on Pressurized Carbonation of Phosphogypsum with High Concentration of CO2*; University of Chinese Academy of Sciences, 2016.
(24) Abdel-Aal, E. A.; Rashad, M. M.; El-Shall, H. Crystallization of Calcium Sulfate Dihydrate at Different Supersaturation Ratios and Different Free Sulfate Concentrations. *Cryst. Res. Technol.* **2004**, *39*, 313−321.
(25) Abdel-Aal, E. A. Crystallization of phosphogypsum in continuous phosphoric acid industrial plant. *Cryst. Res. Technol.* **2004**, *39*, 123−130.
(26) da Silva, N. M. P.; Rong, Y.; Espitalier, F.; Baillon, F.; Gaunand, A. Solvothermal Recrystallization of α-Calcium Sulfate Hemihydrate: Batch Reactor Experiments and Kinetic Modelling. *J. Cryst. Growth* **2017**, *472*, 46−53.
(27) Sindelar, M. E.; Wolkowski, R. P. Reducing Water-Soluble Phosphorus in Soil through Flue Gas Desulfurization Gypsum Application: Year of Application Effects at Multiple Sites in Wisconsin. *J. Environ. Qual.* **2019**, *48*, 654−659.
(28) Batchu, N. K.; Binnemans, K. Effect of the diluent on the solvent extraction of neodymium(III) by bis(2-ethylhexyl)phosphoric acid (D2EHPA). *Hydrometallurgy* **2018**, *177*, 146−151.
(29) Ma, S. Q.; Li, C. W.; Pu, Z. Y. Discussion on the process of hemihydrate dihydrate dilute phosphoric acid. *Phosphate Compd. Fert.* **2021**, *36*, 30−33.
(30) Yan, F. W.; Zhang, S. F.; Guo, C. Y.; Zhang, X. H.; Chen, G. C.; Yan, F.; Yuan, G. Q. Influence of stirring speed on the crystallization of calcium carbonate. *Cryst. Res. Technol.* **2009**, *44*, 725−728.
(31) Tang, S.; Ji, Y.; Ge, K. Crystallization Kinetics and Mechanisms of Calcium Sulfate Dihydrate: Experimental Investigation and Theoretical Analysis. *Ind. Eng. Chem. Res.* **2020**, *59*, 21676−21684.
(32) Merwe, E. M.; Strydom, C. A.; Potgieter, J. H. Thermogravimetric Analysis of the Reaction Between Carbon and $CaSO_4$·$2H_2O$, Gypsum and Phosphogypsum in an Inert Atmosphere. *Thermochim. Acta* **1999**, *340-341*, 431−437.
(33) Yang, C. Y.; Wei, Y.; Ye, F. B.; Ding, Y. G.; Wu, Y. X. Effect of Additives on Thermal Decomposition of Phosphogypsum. *Adv. Mater. Res.* **2011**, *415-417*, 735−740.
(34) Ma, L. P.; Niu, X. K.; Hou, J.; Zheng, S. C.; Xu, W. J. Reaction Mechanism and Influence Factors Analysis for Calcium Sulfide Generation in the Process of Phosphogypsum Decomposition. *Thermochim. Acta* **2011**, *526*, 163−168.
(35) Yan, X. D.; Ma, L. P.; Zhu, B.; Zheng, D. L.; Lian, Y. Reaction Mechanism Process Analysis with Phosphogypsum Decomposition in Multiatmosphere Control. *Ind. Eng. Chem. Res.* **2014**, *53*, 19453−19459.
(36) Amin, M. I.; Ali, M. M.; Kamal, H. M.; Youssef, A. M.; Akl, M. A. Recovery of High Grade Phosphoric Acid From Wet Process Acid by Solvent Extraction with Aliphatic Alcohols. *Hydrometallurgy* **2010**, *105*, 115−119.
(37) Li, X.; Zhu, G. Y.; Gong, X. K.; Li, S. P.; Liu, B. B.; Li, H. Q. Effects of Si/F/K/Na Impurities on the Crystallization of Calcium Sulfate. *Chin. J. Process Eng.* **2018**, *18*, 815−820.
(38) Li, X.; Zhu, G. Y.; Gong, X. K.; Li, S. P.; Xu, W.; Li, H. Q. Occurrence form of impurities in phosphorus rock and the research of acidolysis process. *Spectrosc. Spectral Anal.* **2019**, *39*, 1288−1293.
(39) Jia, R. Q.; Wang, Q.; Luo, T. Reuse of Phosphogypsum as Hemihydrate Gypsum: The Negative Effect and Content Control of H_3PO_4. *Resour, Conserv. Recycl.* **2021**, *174*, No. 105830.
(40) Liu, R. X.; Li, J.; Su, W. R.; Zhang, X. F.; Li, J. W.; Meng, L. Y. FTIR and XPS Analysis Comparison of Activation Mechanism of Ca^{2+} and Fe^{3+} on Quartz. *Spectrosc. Spectral Anal.* **2020**, *40*, 1876−1882.
(41) Tang, M. Z.; Wang, Z. Y.; Wang, Y. S.; Bao, W. J.; Yang, G.; Sun, Y. Analysis of Impurity Phases in Phosphogypsum by EBSD-XPS. *Spectrosc. Spectral Anal.* **2022**, *42*, 136−140.
(42) Ye, C.; Li, J. Wet process phosphoric acid purification by solvent extraction using N-octanol and tributylphosphate mixtures. *J. Chem. Technol. Biotechnol.* **2013**, *88*, 1715−1720.

https://doi.org/10.1021/acsomega.3c01168
ACS Omega 2023, 8, 28122−28132